A METHOD FOR INFRARED DIAGNOSTICS OF A PLASMA AND ITS USE FOR THE INVESTIGATION OF IONIZATION AND RECOMBINATION OF XENON BEHIND THE FRONT OF A SHOCK WAVE

N. A. GENERALOV, V. P. ZIMAKOV and G. I. KOZLOV

Institute of Mechanics Problems, USSR Academy of Sciences

Submitted January 21, 1970

Zh. Eksp. Teor. Fiz. 58, 1928–1937 (June, 1970)

A method is described for the determination of the electron temperature and electron concentration profiles behind the front of a shock wave. It is based on simultaneous measurement of emission and absorption by the ionized gas in the infrared region of the spectrum (λ = 10.6 microns). Results of an experimental investigation of ionization and recombination processes in xenon at T = 8200–9200°K are presented. Good agreement between the experimental data and recombination theory based on a modified Fokker-Planck theory is obtained.

1. INTRODUCTION

THE investigation of the structure of strong shock waves is of interest mostly because of the possibility of obtaining information concerning the elementary processes that lead to the excitation and ionization of gases. The results of numerous investigations[1-8] of ionization relaxation behind the front of shock waves in monatomic gases offer evidence that the mechanism of the ionization processes changes over the length of the relaxation region. Therefore, in the general case, it is possible to separate the following three zones in the development of the ionization process: 1) initial zone, where the formation of the priming electrons takes place; 2) the zone of evolution of the electron cascade in elastic electron-atom collisions; 3) the zone adjacent to the equilibrium region and characterized by the influence of recombination processes on the ionization kinetics.

There are different opinions in the literature concerning the mechanism of formation of electrons in the initial zone of the ionization process; the probable processes considered were atom-atom collisions (including the impurity atoms) and photoionization. Thus, for example, in[5] it was shown that a small admixture of air noticeably influences the time of ionization relaxation in monatomic gases. However, if we consider pure gases with an impurity level less than 10^{-4}, then the formation of priming electrons as a result of atom-impurity processes can be neglected. In this case the mechanism of electron formation in the initial zone will probably depend on the intensity of the shock wave. It is advantageous here to distinguish between (i) weakly ionizing shock waves with clearly pronounced atom-atom zones, (ii) strongly ionizing shock waves when there is practically no atom-atom zone and the formation of priming electrons is due to photo-ionization, while the zone of evolution of the electron cascade is adjacent to the front of the shock wave, and (iii) shock waves having a clearly pronounced pre-frontal structure.

In a number of investigations performed with weakly-ionizing shock waves[3,4] they measured the profiles of the growth of the electron density in the atom-atom zone and showed that in monatomic gases there is realized a two-stage ionization mechanism, in which the atom is first excited, followed by ionization from the excited levels. In this case, the process determining the rate of ionization is the excitation of the atom. As a result, it was possible to determine the cross section for excitation in atom-atom collisions for a number of gases (argon, xenon, krypton).

The laws governing ionization in the zone where the electron cascade developed in electron-atom collisions have been investigated to a lesser degree, this being due to the lack of a reliable method of plasma diagnostics with sufficient sensitivity and time resolution in the region of relatively high electron densities. The difficulty of investigating this region is compounded by the fact that to obtain information on the rate of the ionization process it is necessary to measure, simultaneously with the determination of the profile of the electron density, also the profile of the electron temperature behind the front of the shock wave.

The purpose of the present investigation was indeed to develop such a method and to investigate exhaustively the zones of the development of the electron cascade and of the near-equilibrium zone behind the front of the shock wave in xenon, so as to obtain the values of the ionization and recombination rate constants, and accordingly the cross sections of these processes. The proposed method consists of simultaneously recording the emission and absorption of the plasma behind the shock-wave front in the infrared region of the spectrum (λ = 10.6 μ), making it possible to determine the distribution of the electron density and of the temperature. It is known that in this region of the spectrum the main contribution to the processes of emission and absorption of light are made by free-free transitions of the electrons in the field of the ions. In fact, the ratio of the contributions of the bound-free and free-free transitions, for all atoms, at frequencies below threshold, is approximately $\exp(h\nu/kTe) - 1$, and therefore at a temperature on the order of 1 eV the contribution of the bound-free transitions at a wavelength 10.6 μ is small and can be neglected.

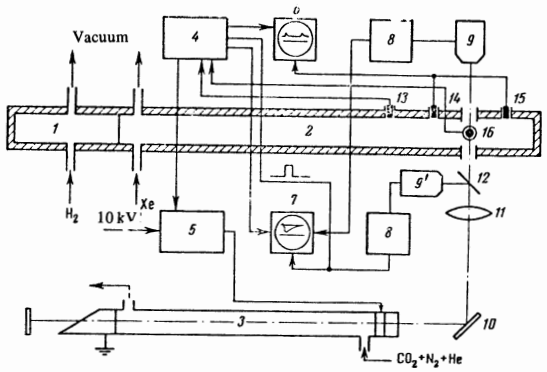

FIG. 1. Diagram of experimental setup; 1, 2—high-and low-pressure chambers, 3—CO_2 gas laser, 4—synchronization system, 5—circuit for shaping the rectangular pulses of laser supply, 6, 7—OK-17M oscilloscopes, 8—amplifiers, 9, 9′—infrared radiation receivers, 10—rotating mirror, 11—gathering lens, 12—NaCl plate, 13, 14, 15—piezoelectric pickups, 16—sighting window on shock tube.

2. EXPERIMENTAL SETUP

An investigation of the kinetics of the ionization behind the front of the shock waves was carried out with an experimental setup consisting of a shock tube, a gas laser (CO_2 + N_2 + He mixture), and a system for recording infrared radiation and measuring of the velocity of the shock waves (Fig. 1). The shock tubes had high and low pressure chambers with inside diameter 80 mm and length 2 and 8.2 m respectively, separated by a diaphragm of annealed copper. The low-pressure chamber was evacuated to a pressure 10^{-3} mm Hg with a forevacuum pump and a diffusion pump through a trap with liquid nitrogen. To reduce the level of the impurities in the shock tube, the latter was "scrubbed" before the experiment by the investigated gas (xenon). The propelling gas was hydrogen or a mixture of hydrogen with a small amount of nitrogen.

The windows through which the infrared radiation of the laser and of the plasma were emitted were located at a distance of 7 m from the diaphragm. The windows were made of single-crystal high-impurity germanium (resistivity larger than 45 ohm-cm) and were sealed in special sockets with the aid of teflon gaskets. The surfaces of the windows were polished and covered on the inside with steel diaphragms having an aperture of ~2 mm. Such diaphragms excluded practically completely the undesirable action of the plasma radiation on the germanium and increased the resolving power of the system. The germanium windows were 6 mm thick, leading to an attenuation of the radiation by a factor 3.5, in the region λ = 10.6 μ, 50% of this loss being due to reflection.

The experiments have shown that neither shock loads nor contact with the plasma cause destruction of the windows or damage to their surfaces.

The gas laser was 3.5 m long and had a tube diameter 57 mm; it operated in the pulse regime with a mixture of CO_2 + N_2 + He continuously drawn through it. The laser resonator consisted of a spherical (internal) and flat (external) mirror. The radiation was extracted through an aperture 6 mm diameter in the spherical mirror. The other end of the laser was covered with a plate of NaCl, mounted at the Brewster angle. The discharge current in the dc regime did not exceed 90 mA, and the radiation power reached 70 W in this case. Under these conditions, appreciable oscillations of the intensity of the radiation were observed. A special electronic circuit was therefore developed, making it possible to obtain single laser pulses of sufficiently large duration and amplitude, and with a smooth top. It turned out that the amplitude, shape, and duration of the pulse of the laser emission depended exceedingly strongly on the composition of the gas mixture, on the discharge voltage, and on the time intervals between pulses. For a certain combination of these parameters, the pulse has a duration on the order of 600 μsec, and an almost flat top.

After reflection from the mirror 10, the laser radiation was focused by lens 11 and entered the shock tube after passing through a NaCl plate mounted at an angle to the beam. The focal length of the lens was 70 cm, so that a practically parallel beam of 1.5—2 mm diameter passed through the shock tube. The use of a plate of NaCl has made it possible to register in one experiment, besides the radiation transmitted through the shock tube, also the form of the initial signal. To exclude the plasma's own radiation in the measurement of its absorptivity, a thin plate of InSb and a teflon film were placed ahead of the receiver 9. The result was a filter with a lower end point 9 μ. The upper end point was determined by the sensitivity of the recording instrument (~10 μ). Simultaneously, the InSb and the teflon film served as attenuators for the laser radiation. At the same time, the filter made up of the indium antimonide and the teflon made it possible to separate the radiation of the plasma in a sufficiently narrow wavelength interval without using a monochromator. The emission was registered with receiver 9 in a second experiment under the same conditions as the absorption.

The registration system consisted of infrared radiation receivers, amplifiers, and OK-17M oscilloscopes. The radiation receivers were photo-resistors based on germanium doped with gold. The resolution time of the sensitive element was 1 μsec. Receiver 9 was used to register the laser radiation passing through the tube, while receiver 9′ was used to determine the waveform of the initial signal. After preliminary amplification, the voltage pulses from receivers 9 and 9′ were fed through cathode followers to the oscilloscope, and were made to overlap by adjusting the gain. The position of the shock-wave front on the absorption signal was noted by a pulse fed from a piezoelectric pickup, which was mounted in the same section as the sighting windows.

The shock wave velocity was measured with two piezoelectric pickups mounted in the measuring section at a distance of 600 mm from each other. The signals from these pickups, together with the calibration time markers, were fed to the second OK-17M oscilloscope.

3. DETERMINATION OF THE ELECTRON DENSITY, TEMPERATURE, AND IONIZATION RATE

The setup described above was used to perform experiments on the determination of the distribution of the absorptivity of the xenon and the intensity of its emission in the infrared region of the spectrum behind the shock-wave front. Typical oscillograms are shown

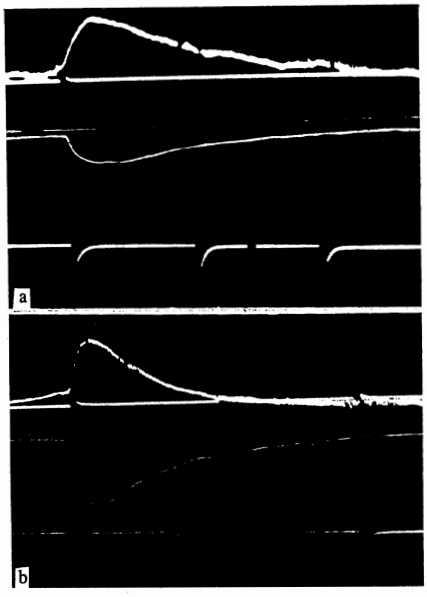

FIG. 2. Oscillograms of emission (top) and absorption (bottom) of xenon in the region of $\lambda = 10.6\mu$, $p_1 = 3$ mm Hg, interval between time markers $\Delta t_L = 66.7$ μsec; a–M = 11.2, b–M = 12.7.

in Fig. 2. On each of the oscillograms are given the distributions of the absorptivity (lower curve) and of the radiation intensity (upper curve). At some instant of time (marked by a pulse from the piezoelectric pickup), the shock-wave front arrives at the sighting windows, followed by a gradual growth of the emission and absorption signals. After a certain time, which depends on the Mach number of the shock wave, these signals reach their maximum values, and subsequently decrease.

Since the emission and absorption of the radiation by the plasma behind the shock-wave front at $\lambda = 10.6\ \mu$ are connected principally with free-free transitions of the electrons, it follows, as will be shown below, that the profile of the square of the electron density duplicates in the main the shape of the oscillograms of the emission and absorption. Bearing this in mind, it is possible to explain the oscillographic curves qualitatively.

The sensitivity of the method developed here does not make it possible to trace the appearance of the electrons in the region of atom-atom collisions, but the region of cascade ionization, accompanied by a sharp increase of the emission and absorption of infrared radiation, is registered with sufficient reliability. The time delay in the appearance of the cascade behind the front of the shock wave depends on the Mach number of the shock wave. After the equilibrium state (the maximum on the oscillographic curves) is reached, the gas begins to cool in time, the density of the electron decreases, and consequently the emission and absorption of the plasma decrease.

Since the time of establishment of the Maxwellian distribution for electrons, under the conditions of our experiments, is approximately 10^{-11} sec, which is much less than the time required to reach equilibrium ionization, we can use Kirchhoff's law for a quantitative analysis of the results.

For a homogeneous plasma layer of thickness l, the connection between the radiation intensity I and the absorption coefficient κ' is given by

$$I(\nu, T_e) = I_{\nu p}(T_e)\,(1 - e^{-\kappa' l}); \tag{1}$$

Here $I_{\nu p}(T_t)$ is the intensity of black-body radiation (erg/cm^2-sec-sr), T_e is the electron temperature, and κ' is the absorption coefficient corrected for the stimulated emission, i.e., $\kappa' = \kappa(1 - \exp[h\nu/kT_e])$, where κ is the true absorption coefficient. It is known that the quantity $1 - e^{-\kappa' l}$ is equal, under the conditions of a continuous spectrum, to the absorptivity of the substance $A(\nu, T_e)$. Therefore expression (1) can be rewritten in the form

$$\frac{I(\nu, T_e)}{A(\nu, T_e)} = \frac{2h\nu^3}{c^2}\frac{1}{e^{h\nu/kT_e} - 1}. \tag{2}$$

Formula (2) will henceforth be used to determine the profile of the electron temperature T_e from the data on the emission and absorption of the plasma. It was assumed here that at the maximum of the oscillographic curves, the temperature T_e is equal to the equilibrium temperature calculated from the conservation law, the equations of state, and the Saha equations.

Knowing the dependence of T_e and κ' on the time, it is possible to determine the electron density profile n_e. To this end we use the formula for the absorption coefficient with allowance for stimulated emission:

$$\varkappa' = \frac{16\pi^2 e^2}{3\sqrt{3}\,ch(2\pi m)^{1/2}}\frac{n_e^2(1 - e^{-h\nu/kT_e})}{(kT_e)^{1/2}}g, \tag{3}$$

where g is the Gaunt factor and the remaining symbols are standard.

Different authors[9,10] give different expressions for the Gaunt factor. However, the calculation based on these formulas for the conditions of our experiment yields approximately the same value ($g \sim 2$).

We now find the connection between the ionization rate $(dn_e/dt)_i$ and the change in the number of electrons behind the front of the shock wave, which is due to two causes—the change of the gas density and the ionization processes. We start from the continuity equation for the j-th component of matter in the volume element:

$$\frac{dn_j}{dt} = \frac{\partial n_j}{\partial t} + v\frac{\partial n_j}{\partial x} = -n_j\frac{\partial v}{\partial x} + \left(\frac{dn_j}{dt}\right)_i, \tag{4}$$

where v is the velocity of the volume element of the gas and $(dn_j/dt)_i$ is the rate of the ionization process.

For a steady-state one-dimensional flux behind the shock wave, from the continuity and energy-conservation equations

$$\rho_1 D = \rho_2 v,$$

$$\frac{5}{2}\frac{k}{m_a}T_1 + \frac{D^2}{2} = \frac{5}{2}\frac{k}{m_a}(T_a + \xi T_e) + \frac{v^2}{2} + \xi\frac{J}{m_a} \tag{5}$$

and the equation of state

$$p = (n_a + n_e)k(T_a + \xi T_e) \tag{6}$$

Under the assumption that $(\rho_1/\rho_2)^2 \ll 1$, $(5/2)kT_1 \ll m_a D^2/2$, and $\xi T_e \ll T_a$, we can obtain the following approximate relation:

$$\frac{dn_e}{dt} = \frac{m_a D^2}{5kT_a}\left(\frac{dn_e}{dt}\right)_i, \tag{7}$$

where ρ_1 and ρ_2 is the density of the gas ahead of the jump and behind it, D is the velocity of the shock wave,

T_1 is the initial gas temperature, m_a is the mass of the atom, n_e and n_a are respectively the electron and atom densities per cm^3, $\xi = n_e/(n_a + n_e)$ is the degree of ionization, J is the ionization potential, and T_a is the atomic temperature, with

$$T_a = T_1\left\{1 - \xi\left(\frac{T_e}{T_1}\right) - \frac{2}{5}\xi\left(\frac{J}{kT_1}\right) + \frac{M^2}{3}\left[1 - \left(\frac{\rho_1}{\rho_2}\right)^2\right]\right\}, \quad (8)$$

where M is the Mach number of the shock wave.

In the general case the derivative $(dn_e/dt)_i$ in Eq. (7) is determined by the aggregate of the collision and radiative excitation and deactivation processes, ionization, and recombination. In an exact determination of the ionization rate it is necessary to consider the system of kinetic equations that determine the populations of all the levels of the atom. However, an analysis carried out by Bates et al.[11] has shown that the populations of the upper excited states reach quasi-equilibrium values very rapidly, so it can be assumed that at any point behind the front of the shock wave the populations of the excited states are connected with the electron density by a modified Saha equation. We shall assume that this holds true for all the excited levels down to the first excited one. At the same time, the population of the ground state will differ from the equilibrium population corresponding to the electron temperature. Thus, the relative population of the ground and first-excited levels will differ from the Boltzmann value.

We note also that the absolute magnitudes of the populations of the excited levels for inert gases are very small, so that it can be assumed that the rate of change of the population of the ground state is equal to the rate of change of the electron density.

Under our conditions $n_e \sim 5 \times 10^{16}$ cm^3. Therefore, in accordance with the Griem criterion[12], the contribution of the radiated transition to the value of $(dn_e/dt)_i$ can be neglected and we can confine ourselves to collision processes. Then

$$(dn_e/dt)_i = \alpha n_e n_a - \beta n_e^3, \quad (9)$$

where α and β are the constants of the ionization and recombination rates, and are connected with one another by the detailed-balancing principle

$$\alpha/\beta = K(T_e), \quad (10)$$

while

$$K(T_e) = \frac{g_+}{g_0}\frac{2(2\pi m_e kT_e)^{3/2}}{h}\exp\left(-\frac{J}{kT_e}\right)$$

is the Saha formula (the symbols here are standard). From (9) and (10) we can obtain for α the following expression:

$$\alpha = \frac{dn_e/dt}{(m_a D^2/5kT_a)\, n_a n_e [1 - n_e^2/n_a K(T_e)]}. \quad (11)$$

It should be borne in mind that the ionization rate constant determined from (11) is actually the rate constant of the excitation from the ground state in electron-atom collisions, since it is precisely this process which determines the ionization rate. Approximating, as usual, the dependence of the excitation cross section of the level E* on the electron energy near the threshold of excitation, by the straight line $\sigma = C_e(E - E^*)$, we can obtain the following expression for the effective excitation cross section C_e, corresponding to an electron energy exceeding E* by 1 eV:

$$C_e = \frac{5kT_a}{2m_a D^2}\sqrt{\frac{\pi m_e}{2kT_e}}\frac{\exp(E^*/kT_e)}{(E^* + 2kT_e)[1 - n_e^2/n_a K(T_e)]n_a n_e}\frac{dn_e}{dt}. \quad (12)$$

From this relation we can determine C_e, if E* is known. The value of E* can be determined experimentally from our data, if the plot of $\ln(\alpha/T_e^{3/2})$ against $1/T_e$ is constructed for a sufficiently wide temperature interval.

It should be noted that the quantity dn_e/dt in formulas (7), (9), (11), and (12) is defined in a system connected with a particle, whereas experiment yields the derivative dn_e/dt_L in the laboratory frame, with $dt = (\rho_2/\rho_1)dt_L$.

4. RESULTS AND THEIR DISCUSSION

The experiments were performed at an initial xenon pressure of 3 mm Hg. The results of the experiments are shown in Fig. 2 for the two most characteristic regimes, with M equal to 11.2 and 12.7. The time intervals between the margins on the oscillograms are 67 μsec of laboratory time. The method described above was used to determine from these oscillograms the profiles of the electronic and atomic temperatures and the distribution of the electron density in the shock waves. The atomic temperature was determined from formula (8). The results of such a reduction are shown in Figs. 3 and 4. It is easy to see that the atomic temperature decreases quite sharply in the ionization process, while the electronic temperature increases insignificantly, approaching the atomic temperature in the equilibrium region. This is in agreement with the theoretical calculations of[7], where it is indicated that the electron temperature in a xenon plasma behind the front of the shock wave is equal to the equilibrium atomic temperature. It follows from Fig. 3 that actually at $M < 12.7$ the electron temperature is practically always equal to the equilibrium atomic temperature. With increasing intensity of the shock waves, the changes of the temperatures T_e and T_a increase. After the equilibrium state of the gas is reached, its temperature (now $T_e = T_a$) begins to decrease, owing to the cooling of the plasma as a result of radiation losses. This cooling reaches its largest value at M = 12.7, where the temperature of the plasma drops by 600°K within 50 μsec of laboratory time. We note that at M = 11.2, during the same time interval, the plasma cools only by 200°K.

The distribution of the electron density in the shock

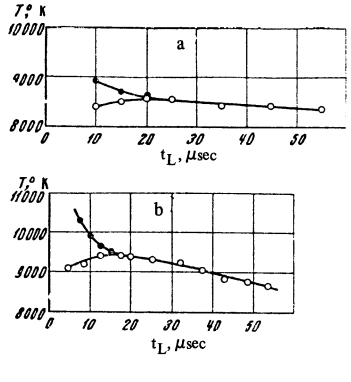

FIG. 3. Distribution of the electronic temperature T_e(●) and of the atomic temperature T_a(○) behind the front of a shock wave in xenon. p_1 = 3 mm Hg (laboratory time); a–M = 11.2, b–M = 12.7.

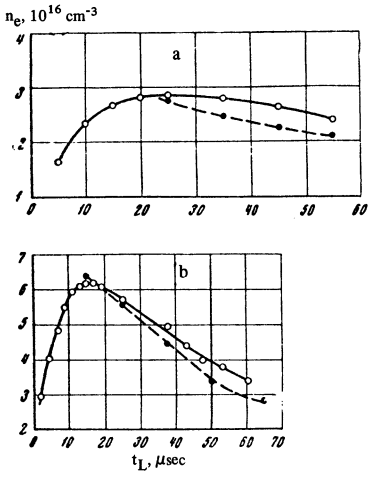

FIG. 4

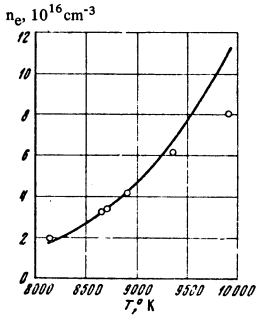

FIG. 5

FIG. 4. Distribution of electron density behind the front of a shock wave in xenon; p_1 = 3 mm Hg. (laboratory time); O–experiment, ●–Saha equations; a–M = 11.2, b–M = 12.7.

FIG. 5. Temperature dependence of equilibrium concentration of electrons in xenon; p_1 = 3 mm Hg; points–experimental values, curve–calculation result.

wave also passes through a maximum. The drop of the electron density after the equilibrium values are reached is also connected with radiative cooling of the plasma. The form and the position of the maxima of the electron density depend in this case on the intensity of the shock waves; at M = 12.7 the maximum turns out to be more strongly pronounced, whereas at M = 11.2 the gradients of the electron density are much smaller in magnitude. It must be noted first of all that the experimental equilibrium values of the electron density are in good agreement with the calculated values based on the shock adiabat, as can be seen from the data shown in Fig. 5. At T > 9000°K, the experimental values turned out to be somewhat smaller, and this may possibly be connected with the influence of radiative losses. Figure 4 shows the total profiles of the electron density, including the region where it decreases after reaching the maximum. It has turned out here that the experimental values are also in satisfactory agreement with the calculated values of the electron density obtained from the Saha equation using the experimental temperature profile.

Using the obtained profile of the electron density and the electron temperature T_e behind the front of the shock wave, we have determined with the aid of formula (11) the values of the ionization rate constant α in the electron temperature interval 8200–9200°K. The results of these measurements are shown in Fig. 6, from which it is seen that α increases rapidly with increasing temperature. If we plot $\ln(\alpha/T_e^{3/2})$ against $1/T_e$ (Fig. 7), then we can easily obtain the activation energy E* of the ionization process. It turns out to equal (8.4 ± 0.4) eV, corresponding to the excitation energy of the first electronic level of the xenon atom. Knowing the activation energy of the ionization processes, we can determine the second parameter in the expression for the excitation cross section, C_e. To this end, we use formula (12) and the distributions of n_e and T_e behind the shock-wave front. The values of C_e obtained in this manner at

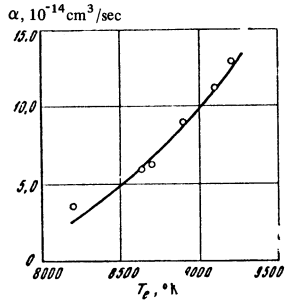

FIG. 6

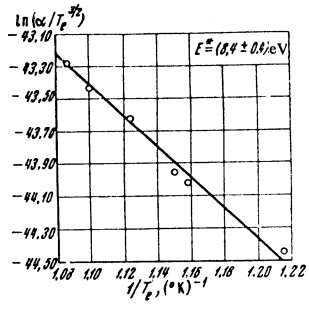

FIG. 7

FIG. 6. Dependence of the ionization rate constant of xenon on the electron temperature.

FIG. 7. Dependence of $\ln(\alpha/T_e^{3/2})$ on $10^4/T_e$ in xenon.

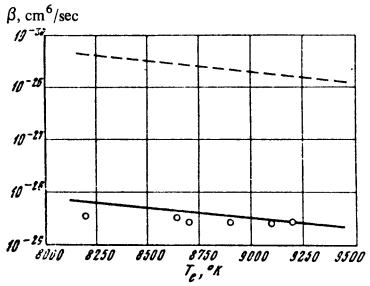

FIG. 8. Temperature dependence of the recombination rate constant of Xe^+ in triple collisions: points–experimental values, solid curves–theoretical value [17], dashed–theoretical value [14].

T_e = 8200–9200°K turn out to be approximately the same: $(5.7–5.8) \times 10^{-18}$ cm^2/eV. This is approximately one-third the value recently obtained in[13] for the total cross section for inelastic electron-atom collisions in xenon.

The coefficients α and β are connected by relation (10), making it possible to calculate the recombination coefficient. It turned out that in the temperature interval 8200–9200°K the value of β changes in the range $(3.6–2.8) \times 10^{-29}$ cm^6/sec.

It is of interest to compare the values of the recombination coefficient obtained in this manner with the theoretical values.

In the theoretical analysis of the recombination process, there are two approaches. In the first[11,14] one solves the system of balance equations for the levels of the atom, assumed to be discrete, while in the second[15,16] the recombination is regarded as a Brownian motion of the electron in continuous energy space. In[17] a modified diffusion approximation is used, in which the discrete structure of the energy spectrum is retained.

The results of[15,16] pertain to the region of sufficiently low temperatures (T < 3000°K), so that the experimental data will be compared with the conclusions of[14,17] (Fig. 8). It follows from the analysis of Fig. 8 that the experimental values of β, obtained in this paper, are in good agreement with the conclusions of the theory of Biberman, Vorob'ev, and Yakubov[17] and deviate greatly (by three orders of magnitude) from the calculations of Chen[14], carried out in accordance with the scheme of Bates, Kingston, and McWhirter[11].

In conclusion, the authors are deeply grateful to Yu.

P. Raizer for a discussion of the results and to V. I. Fotiev and A. É. Abaliev for help with the work.

[1] H. Petcheck and S. Byron, Ann. of Phys. 1, 270 (1957).
[2] H. S. Johnston and W. M. Kornegay, Trans. Faraday Soc. 57, 1563 (1961).
[3] K. E. Harwell and R. G. Jahn, Phys. of Fluids 27, 214 (1964).
[4] A. J. Kelly, J. Chem. Phys. 45, 1723 (1966).
[5] G. I. Kozlov, Yu. P. Raĭzer, and D. I. Roĭtenburg, Prikl. Mat. Teor. Fiz. 1, 140 (1968).
[6] T. I. McLaren and R. M. Hobson, Phys. of Fluids 11, 2162 (1968).
[7] J. A. Smith, Phys. of Fluids 11, 2150 (1968).
[8] G. K. Tumakaev and V. R. Lazovskaya, VIII Intern. Conf. on Phenomena in Ionized Gases, Vienna, 1968.
[9] C. W. Allen, Astrophysical Quantities, Oxford Univ. Press, 1963.
[10] W. L. Karsas and R. Latter, Astrophys. J. Suppl. 6, 167 (1961).
[11] D. R. Bates, A. E. Kingston, and R. W. P. McWhirter, Proc. Roy. Soc. A267, 297 (1962).
[12] H. Griem, Plasma Spectroscopy, McGraw, 1964.
[13] A. J. Dixon and A. Von Engel, Int. J. Electronics 25, 233 (1968).
[14] C. J. Chen, J. Chem. Phys. 50, 1560 (1969).
[15] L. P. Pitaevskiĭ, Zh. Eksp. Teor. Fiz. 42, 1326 (1962) [Sov. Phys.-JETP 15, 919 (1962)].
[16] A. V. Gurevich and L. P. Pitaevskiĭ, ibid. 46, 1281 (1964) [19, 870 (1964)].
[17] L. M. Biberman, V. S. Vorob'ev, and I. T. Yakubov, ibid. 56, 1992 (1969) [29, 1070 (1969)].

Translated by J. G. Adashko
237